Macromolecules

Volume 33, Number 20 October 3, 2000

Communications to the Editor

Shear Orientation of Viscoelastic Polymer−Clay Solutions Probed by Flow Birefringence and SANS

Gudrun Schmidt,*,† Alan I. Nakatani,† Paul D. Butler,‡ Alamgir Karim,† and Charles C. Han†

Polymers Division and Center for Neutron Research, National Institute of Standards and Technology, Gaithersburg, Maryland 20899

Received November 8, 1999
Revised Manuscript Received April 24, 2000

Shear-induced structural changes in complex fluids of anisotropic species are a very general problem encountered not only in polymer solutions[1] but also in liquid crystalline materials,[2,3] block copolymer melts,[1,4,5] and platelike clay suspensions.[6−11] Different experimental techniques such as flow birefringence and small angle scattering have been developed to monitor such shear-induced structural changes.[12,13] Since shear can influence both the texture and the orientation of the underlying anisotropic species, it is helpful to combine different techniques in order to obtain information on different length scales. The objective of this contribution is to investigate the influence of shear on the structure of a highly viscoelastic clay−polymer solution. Previous investigations proposed many structural models to explain the mesoscopic properties[14−19] and shear behavior of aqueous clay solutions.[20−22] Despite a large body of literature on the flow behavior of polymer solutions,[1,23] little is known about the influence of shear on the viscoelastic clay−polymer solutions related to nanocomposite materials.[24]

In this study an aqueous solution of the synthetic hectorite type clay, Laponite, LRD (Laporte Industries Ltd),[25] and poly(ethylene oxide), PEO was investigated under shear by flow birefringence and small-angle neutron scattering. The clay particles are composed of platelets of high purity and uniform crystallite size (300 Å in diameter and ca. 10 Å thick).[26,27] Poly(ethylene oxide) with a $M_w = 10^6$ g/mol[28] was purchased from Polysciences Inc.[25] For all samples in this study, a pH value of 10 and a NaCl concentration of 10^{-3} mol/L were used. The results reported here were obtained on a solution containing mass fractions of 3% LRD and 2% PEO at room temperature.[28]

Birefringence experiments were performed at 25 °C on a Rheometrics Scientific[25] SR 5000 rheometer with an integrated rheo-optical module. The rheometer is equipped with a 3.8 cm diameter quartz parallel plate geometry, with the incident laser beam parallel to the direction of the shear gradient (1−3 plane). For all birefringence experiments a gap of 1 mm was used.

Prior to shear, the sample is transparent and isotropic. Constant shear rates were applied for ca. 4000 s at low shear rates ($d\gamma/dt < 5\ s^{-1}$) and ca. 1000 s at higher shear rates ($d\gamma/dt > 5\ s^{-1}$). These intervals were sufficient to reach a steady state as determined from both the time dependent viscosity and birefringence measurements. The shear rate dependence of viscosity and birefringence was obtained by performing individual, time-dependent, constant rate experiments. Once the samples equilibrated after cessation, another time-dependent, constant rate experiment was performed. The steady-state values of viscosity and birefringence as a function of shear rate are shown in Figure 1. The solution shear thins over the entire range of shear rates as shown by a double logarithmic plot of η versus shear rate, $d\gamma/dt$, (Figure 1, insert) and gives a power law exponent, ($m = -0.65$ ($\eta = (d\gamma/dt)^m$). A minimum in the birefringence is observed at a critical shear rate, $(d\gamma/dt)_{critical}$, ca. 40 s^{-1} (Figure 1). While the birefringence displays a distinct minimum, the viscosity shows no corresponding feature at the critical shear rate.

* To whom correspondence should be sent.
† Polymers Division, National Institute of Standards and Technology.
‡ Center for Neutron Research, National Institute of Standards and Technology.

10.1021/ma9918811 This article not subject to U.S. Copyright. Published 2000 by the American Chemical Society
Published on Web 09/13/2000

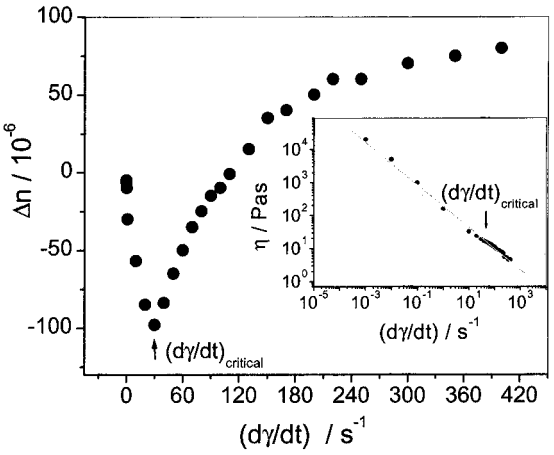

Figure 1. Steady-state values of birefringence, Δn, as a function of shear rates. The relative error in the steady-state birefringence is ca. ±4%. Inset: Steady-state viscosity as a function of shear rates. The double logarithmic plot gives a power law exponent of −0.65. The relative error on steady state values is approximately ±5%.

Birefringence is due to anisotropies of the refractive index in the sample.[12,29] When the sample is free of stress and the polymer chains and clay platelets are randomly oriented, the total refractive index, n, will be isotropic. With increasing shear rate, we first observed a decrease in birefringence. According to SANS from contrast matched samples, the polymer chains themselves do not orient significantly at shear rates less than 30−40 s^{-1}.[30] Therefore, at these shear rates, the only anisotropic component in the solution is the clay. The clay platelets orient in the shear field, which leads to an anisotropy in the refractive index and therefore the birefringence. A disklike particle will have three principal symmetry axes and therefore three refractive index components. Two of the axes are equivalent due to the geometry of the platelet. The third symmetry axis is normal to the disk plane. The contribution to birefringence from the clay particles can be negative, according to literature[13,31] and experiments on aqueous clay solutions.[30] However, Shah et al.[31] showed that the sign of steady state (electric) birefringence of clay suspensions (montmorillonite) at low fields reverses from negative to positive with an increase in field strength. He proposed that the disk-shaped particles possess an electric permanent dipole moment along the normal to the disk plane and a field-induced dipole moment. Yamaoka et al.[32] argued against the proposition of Shah that the clay particle should possess no intrinsic permanent dipole moment directed normal to the plane of disklike layers.

From our negative birefringence data alone, we cannot determine how the platelets are oriented along the flow direction since the total birefringence may consist of intrinsic and form birefringence of clay platelets and polymer chains. SANS is useful in determining the orientation of the polymer−clay system under shear.

SANS utilized the 30 m SANS instrument on NG7 at the National Institute of Standards and Technology Center for Neutron Research.[33] The shear cell is a Couette geometry, which has been described previously.[34] The cell has an inner diameter of 60 mm and a gap of 0.5 mm giving a total path length of 1 mm through the sample. In the standard configuration, referred to as the "radial beam" geometry, the incident beam is parallel to the shear gradient. In a second configuration, referred to as the "tangential beam" geometry, the incident beam is parallel to the flow direction. A sample to detector distance of 11.25 m and an incident wavelength, λ, of 9 Å was used to give a q range ($q = 4\pi/\lambda \sin(\theta)/2$) of 0.0027 $Å^{-1} < q < 0.0199$ $Å^{-1}$. The primary contrast in the SANS experiment is between D_2O and the other solution components (clay, PEO, salts); thus, SANS experiments can detect the orientation of the clay platelets and polymer chains under shear. SANS on contrast matched samples (to clay) detect only the orientation of the polymer. These experiments will be discussed in more detail in a later publication.[30]

The results (raw data) obtained from the polymer−clay solutions in the "radial" and "tangential" beam configurations are summarized in Figure 2. The apparent anisotropy is lower in tangential beam due to the distribution of platelets caused by the curvature of the shear cell in the tangential scattering geometry. At rest, a diffuse isotropic ring of scattering intensity was observed which becomes more diffuse at low shear rates (Figure 2a). The ring corresponds to an average spacing between platelets $q_{max} \approx 0.007$ $Å^{-1}$, 3% w/w clay ($d = 2\pi/q_{max} = 900-1100$ Å). Recent work of Saunders et al.[35] on unoriented Laponite gels under similar conditions showed a structure factor maximum at 0.014 $Å^{-1}$ (4% w/w) and 0.02 $Å^{-1}$ (6% w/w). Compared to our results, the interparticle distance observed in this study is consistent with their results. With increasing shear rate, the ring disappears, no maximum is retained in the vertical direction and an anisotropic scattering pattern (streak) developed (Figure 2b,c,f). If we neglect the main reflected beam, which appears as a background streak in the gradient direction for tangential beam measurements, the anisotropy pattern increases in the radial and tangential beam measurements, with increasing shear rate. This is indicated by the scattering streaks parallel to the neutral axis of the flow field. After cessation of shear, anisotropic SANS patterns relaxed to an isotropic state in less than 2 min.

To account for the SANS and birefringence results, we propose that the polymer chains must be adsorbed to the clay particles. A 2% solution of PEO, at the same pH, polymer and salt concentration produced no anisotropic SANS patterns and no significant birefringence ($\Delta n \approx 2\ (\pm 0.5) \times 10^{-6}$) was observed at shear rates up to 100 s^{-1}. Similarly a 3% aqueous clay solution showed no anisotropy in the SANS patterns during shear and slight negative birefringence ($\Delta n \approx -12\ (\pm 8) \times 10^{-6}$). The birefringence is less negative than the minimum birefringence of the clay−polymer solution (Figure 1). Therefore, we conclude that the birefringence observed in the clay−polymer solutions is due to a mechanical coupling between clay platelets and polymer, allowing a higher birefringence than either single component in solution can produce. At shear rates less than $(d\gamma/dt)_{critical}$, the decreasing total birefringence indicates that the Δn contribution of clay platelets is dominant. At $(d\gamma/dt)_{critical}$, the birefringence of the stretched polymer chains starts to affect the total birefringence value. The contribution to birefringence from stretched polymer chains, will be positive with chains oriented in flow direction.[12,13] At this point, the anisotropic SANS patterns from contrast matched samples demonstrate that polymer chains start to orient. Above $(d\gamma/dt)_{critical}$ the orientation of the clay continues to increase as well as the Δn contribution of the stretched polymer, therefore

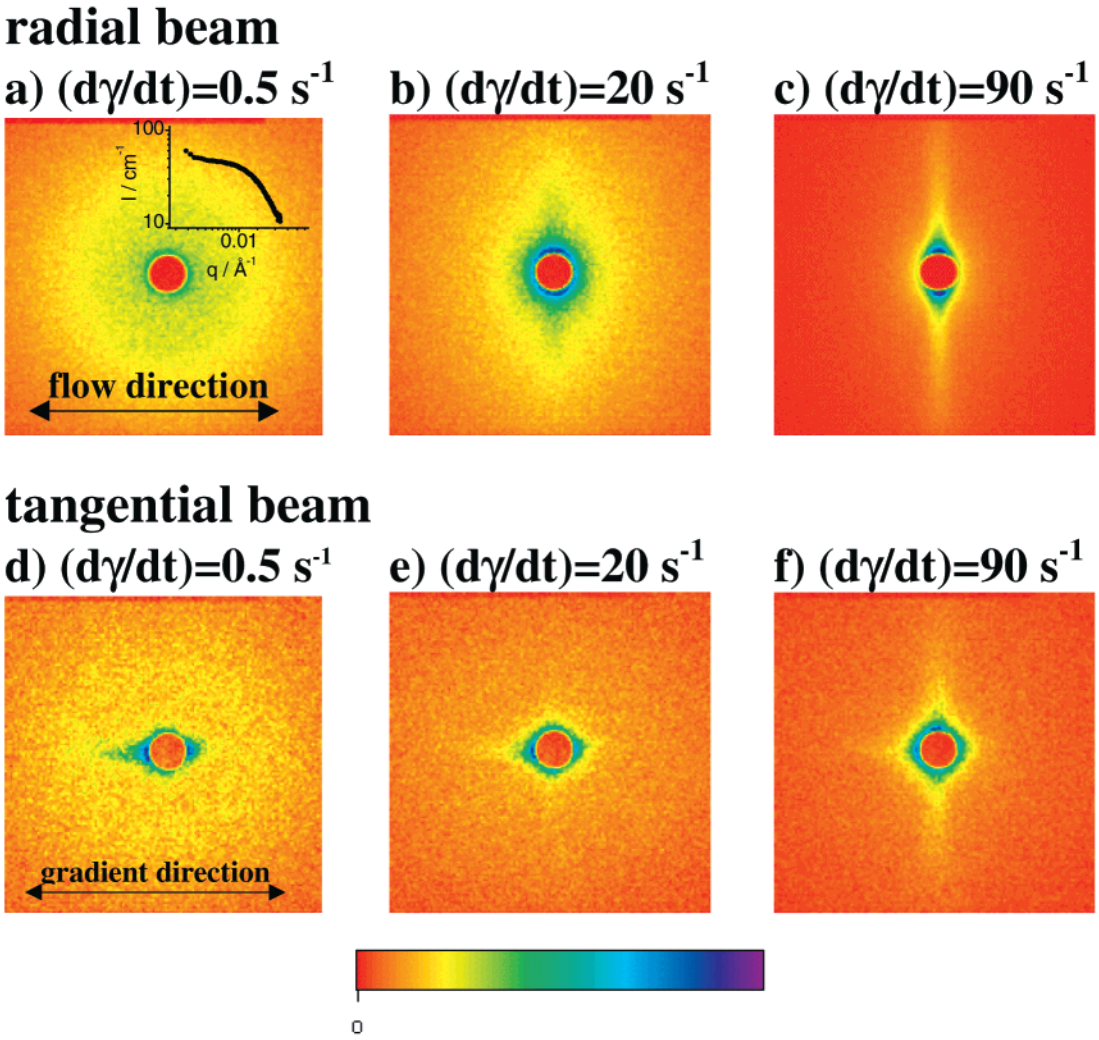

Figure 2. Two-dimensional SANS profiles (raw data) obtained with the radial beam (a−c) and the tangential beam (d−f) at designated shear rates. Anisotropy in gradient direction as observed in parts d−f comes from reflections due to the empty Couette shear cell in the "tangential beam" configuration.

the total birefringence becomes positive.

The SANS data indicate the flow is strong enough to enhance and maintain a continuous increase in the orientation of the polymer−clay system. Platelets can be oriented in three different ways.

1. With the surface normal along the velocity direction.
2. With the surface normal along the flow direction.
3. With the surface normal along neutral direction.

According to SANS patterns from both beam configurations (Figure 2) the shear flow results in an alignment of clay platelets within aggregates ($d = 2\pi/q$ and 2327 Å > d > 315 Å). The platelets are oriented in the flow direction with the surface normal in the neutral direction (Figure 3). This orientation is also occasionally observed in liquid crystalline lamellar phases,[3] block copolymer solutions[36] and melts.[37] The recovery from the SANS anisotropy is much faster than expected from simple Brownian motion of only the clay particles in a medium of the same viscosity as the clay polymer solution exhibited macroscopically, and is indicative of the dynamic coupling of the polymer chains to the clay.

Acknowledgment. Financial support by the Alexander von Humboldt Stiftung is gratefully acknowledged by G.S. We thank Ms. C. Evans of Southern Clay Products for supplying Laponite samples, J. Aarons for providing Figure 3 and E. Amis, R. Ivkov, K. Migler, and J. Douglas for fruitful discussions.

References and Notes

(1) Nakatani, A. I.; Dadmun, M. D. *Flow-induced Structure in Polymers*; ACS Symposium Series 597; American Chemical Society: Washington, DC, 1995.
(2) Jamieson, A. M.; Gu, D. F.; Chen, F. L.; Smith, S. *Prog. Polym. Sci.* **1996**, *21*, 981.
(3) Roux, D.; Nallet, F.; Diat, O.; *Europhys. Lett.* **1993**, *24*, 53.
(4) Nakatani, A. I.; Morrison, F. A.; Jackson, C. L.; Douglas, J. F.; Mays, J. W.; Muthukumar, M.; Han, C. C. *J. Macromol. Sci. Phys.* **1996**, *B35*, 489.
(5) Bates, F. S.; Koppi, K. A.; Tirrell, M.; Almdal, K.; Mortensen, K. *Macromolecules* **1994**, *27*, 5934.
(6) Ramsay, J. D. F. *J. Colloid Interface Sci.* **1986**, *109*, 2, 441.
(7) Mourchid, A.; Delville, A.; Levitz, P, *Faraday Discuss.* **1995**, *101*, 275.
(8) Rand, B.; Melton, I. E. *J. Colloid Interface Sci.* **1977**, *60*, 308.
(9) Melton, I.; Rand, B. *J. Colloid Interface Sci.* **1977**, *60*, 321.
(10) Clarke, S. M.; Rennie, A. R.; Convert, P. *Europhys. Lett.* **1996**, *35*, 233.
(11) Brown, A. B. D.; Ferrero, C.; Narayanan, T. *Eur. Phys. J. B* **1999**, *11*, 481.
(12) Janeschitz-Kriegl. *Polymer Melt Rheology and Flow Birefringence*, Springer-Verlag: Berlin, Heidelberg, Germany, and New York, 1983.
(13) Fuller, G. G.; *Optical Rheometry of Complex Fluids*, Oxford University Press: Oxford, England, 1995.

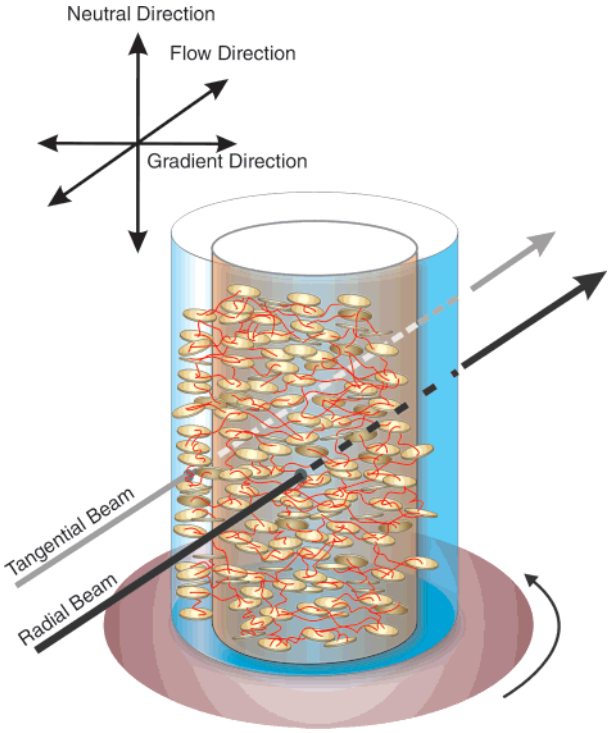

Figure 3. Couette type shear cell for SANS and model for real space orientation of oriented clay platelets in the Couette cell. The reference coordinate frame is anchored in the tangential beam.

(14) Van Olphen, H. *An Introduction to Clay Colloid Chemistry*, Wiley-Interscience: New York, 1977.
(15) Lockhart, N. C. *J. Colloid Interface Sci.* **1980**, *74*, 509.
(16) J. Fripiat, J. Cases, M. Francois, M. Letellier, *J. Colloid Interface Sci. 89*, 378 1982.
(17) Rosta, L.; Von Gunten, H. R. *J. Colloid Interface Sci.* **1990**, *134*, 397.
(18) Ramsay, J. D. F.; Lindner, P. *J. Chem. Soc., Faraday Trans.* **1993**, *89*, 4207.
(19) Morvan, M.; Espinat, D.; Lambard, J.; Zemb, Th. *Colloids Surf.* **1994**, *A 82*, 193.
(20) Mourchild, A.; Delville, A.; Lambard, J.; Lecolier, E.; Levitz, P. *Langmuir* **1995**, *11*, 1942.
(21) Hanley, H. J. M.; Straty, G. C. *Langmuir* **1994**, *10*, 3362.
(22) Pignon, F.; Magnin, A.; Piau, J. M. *J. Rheol.* **1998**, *42*, *6*, 1349.
(23) Marucci, G.; Greco, F. *Adv. Chem. Phys.* **1993**, 86.
(24) Rossi, S.; Luckham, P. F.; Zhu, S. *Rev. I Fr. Pet.* **1997**, *52*, *2*, 199.
(25) Certain equipment and instruments or materials are identified in this paper in order to adequately specify the experimental details. Such identification does not imply recommendation by the National Institute of Standards and Technology nor does it imply the materials are the best available for the purpose.
(26) Ramsay, J. D. F.; Swanton, S. W.; Bunce, J.; Chem, *J. Soc. Faraday Trans.* **1990**, *86*, 3919.
(27) Pignon, F.; Magnin, A.; Piau, J. M.; Cabane, B.; Lindner, P.; Diat, O. *Phys. Rev. E* **1997**, *56*, *3*, 3281.
(28) According to ISO 31−8, the term "Molecular Mass" has been replaced by "Relative Molecular Mass", symbol M_r. Thus, if this nomenclature and notation were to be followed, one would write, M_rw, instead of the historically conventional M_w for the mass average molecular weight and it would be called the "Mass Average Relative Molecular Mass". The conventional notation rather than the ISO notation has been employed for this publication.
(29) Azzam, R. M. A.; Bashara, N. M. *Ellipsometry and Polarized Light*; North Holland: Amsterdam, 1987.
(30) Schmidt, G.; Nakatani, A. I.; Butler, P. D.; Han, C. C. Viscoelastic Polymer−Clay Solutions. Manuscript in preparation.
(31) Shah, M.; Thomson, D. C.; Hart, C. M. *J. Phys. Chem.* **1963**, *67*, 1170.
(32) Yamaoka, K.; Sasai, R.; Ikuta, N. *Chem. Lett.* **1994**, 563.
(33) Glinka, C. J.; Barker, J. G.; Hammouda, B.; Krueger, S.; Moyer, J. J.; Orts, W. J. *J. Appl. Crystallogr.* **1998**, *31*, 430.
(34) Straty, G. C.; Hanley, H. J. M.; Glinka, C. J. *J. Stat. Phys.* **1991**, *62*, 1015.
(35) Saunders, J. M.; Goodwin, J. W.; Richardson, R. M.; Vincent, B. *J. Phys. Chem. B* **1999**, *103*, 9211.
(36) Kitade, S.; Ochiai, N.; Takahashi, Y.; Noda, I.; Matsushita, Y.; Karim, A.; Nakatani, A. I.; Kim, H.; Han, C. C. *Macromolecules* **1998**, *31*, 8083.
(37) Wiesner, U. *Macromol. Chem. Phys.* **1997**, *198*, 3319.

MA9918811